Current Research in Health Sciences, 4(1):24–33, 2026. DOI: 10.58613/crhs415

Current Research in Health Sciences

ISSN (Online): 2584-1084

Journal homepage: https://gpub.org/journal-details.php?journal-id=47

Research Article

In Silico Evaluation of Pharmacokinetic Properties and Drug Likeness of Statins Targeting Histone deacetylase

Mohammed Zuheir Hassan[1], Ahmed Ridha Abduljawad [2], Jawad Kadhim Alshams[3], Dhurgham Qasim Shaheed[3,4] and Ali Jabbar Radhi [3,4*]

[1]*Department of Aesthetic and Laser Techniques, College of Health and Medical Technology, University of Alkafeel, Najaf, Iraq.*
[2]*Faculty of Medical Technologies, Islamic University, Najaf, Iraq.*
[3]*College of Pharmacy, University of AlKafeel, Najaf, Iraq.*
[4]*ARCPMS University of AlKafeel, Najaf, Iraq.*
[*]*Corresponding author: alijebar56@alkafeel.edu.iq*

Article Info

Keywords: *Drug repurposing, Statins, Histone deacetylase 3, Vorinostat, Molecular docking, Structure activity relationship (SAR), ADMET prediction, Pharmacokinetic profiling.*

Received: *12.05.2026;*
Accepted: *19.06.2026;*
Published: *26.06.2026*

Abstract

Drug repurposing holds great potential in terms of discovering new anticancer agents via assigning new therapeutic uses to already approved drugs. Through epigenetic regulation of gene expression, histone deacetylase 3 (HDAC3) functions with great importance in the progression of breast cancer making it an attractive molecular target. We report a full in silico profiling of selected statins (Atorvastatin, Fluvastatin, Pitavastatin, Pravastatin, and Rosuvastatin) as potential HDAC inhibitors compared to the Histone deacetylase 3 crystal structure (PDB ID: 4LXZ) and reference inhibitor Vorinostat. Molecular docking results reveal that all of the evaluated statins dock in the HDAC catalytic pocket and interact with the catalytic Zn_2^+ ion. Atorvastatin showed the best binding affinity (-10.93 Kcal.mol^{-1}) followed by Vorinostat (-8.51 Kcal.mol^{-1}) and stable metal coordination most likely hydrogen bonding and series of π–π interactions with the active-site residues. Structure–activity relationship analyses revealed that both hydrophobic surface area, aromatic moieties and accessibility of the carboxylate zinc-binding group have a major effect on binding stability. Full ADMET profile showed good pharmacokinetic characteristics for most statins, with high predicted absorption from the gut, moderate distribution, amenable metabolic profiles, and generally acceptable toxicity predictions, although atorvastatin showed possible AMES positivity and hERG II inhibition. These computational studies indicate that statins appear to act as very weak non-classical HDAC inhibitors, especially Atorvastatin, consistent with the concept of repurposing these drugs as possible epigenetic anticancer agents.

1. Introduction

Cancer among the leading [1, 2] causes of death around the world. Of the several forms of cancer, breast cancer is the mostly diagnosed cancer worldwide, with over 685,000 deaths and more than 2.3 million cases recorded in 2020. Among the breast cancer subtypes, the hormone receptor (HR) positive is the most commonly detected, followed by the human epidermal growth factor receptor 2 (HER2) positive and triple negative (TN) phenotype. Breast cancer is a highly heterogeneous disease characterized by differences in epigenomic, genomic, proteomic and transcriptomic features of cancer cells [3]. It has been addressed that epigenetic modifications like histone modifications (HMs) and DNA methylation are involved in breast cancer [4]. Histone deacetylases (HDACs) are a family of specific enzymes that catalyze the removal of acetyl groups from the ε-amino group of the proteinogenic histone lysine residues, leading to a tighter chromatin condensation

How To Cite: M.Z. Hassan, A.R. Abduljawad, J.K. Alshams, D.Q. Shaheed and A.J. Radhi. In Silico Evaluation of Pharmacokinetic Properties and Drug Likeness of Statins Targeting Histone deacetylase. *Current Research in Health Sciences*, 4(1):24–33, 2026. https://doi.org/10.58613/crhs415

and thus to a suppression of gene transcription [5]. It has been demonstrated that HDAC can induce as well as promote the development of breast cancer by changing the expression of genes and protein activity. A study by Cui et al. revealed that HDAC3 of the HDAC family is negatively correlated to (reported as associated with low) expression of estrogen receptor and progesterone receptor, but positively correlated with overexpression of human epidermal growth factor 2 and clinical stage of breast tumours [6]. In view of these correlations, the authors recognised HDAC3 to be a prognostic marker in invasive ductal breast cancer. In a separate study by Kim et al. discovered that HDAC3 interacts with CREB3 (specific HDAC3-associated protein) and represses the expression of this target gene [7], thus revealing the ability of this epigenetic enzyme to impair gene transcription since CREB3-mediated CXCR4 transcription will be downregulated, that impedes the MDA-MB-231 cells' triple-negative breast cancer cell line migration, hence indicates the unique role of HDAC3 promoting breast cancer cells [8]. Blessed with selectivity and specificity, this enzyme has been known to be a potential and promising target to combat breast cancer cells. Over the years, several novel HDAC3 inhibitors from nature, i.e. plants and animals, discovered and being used for breast cancer chemotherapy [9]. Like every other drug candidate, those mentioned above have to undergo all the stages of drug discovery, namely the pre-discovery stages (in vitro & in vivo) as well as most importantly clinical trials, to be approved and marketed to the public. This can take more than 15 years from discovery to approved drug [10]. Drug repurposing is an alternative that can help close the Years discovery of novel HDAC3 inhibitors. It refers to the identification of new uses of existing drugs, both those approved by the FDA and across the whole world. This relatively new strategy allows for significantly shorter drug development times and reduced time to market typically for approved repurposed drugs, and hence already likely to be subject to accelerated clinical trials since the drugs have already been evaluated in terms of safety and toxicological clinical studies [11]. Machine learning (ML) refers to a broad class of computational methods that have been integrated into the process of drug discovery across a variety of applications ranging from de novo drug design and target identification, ligand-based screening and ligand optimization to assist and hasten the traditionally lengthy drug discovery process by "thinning the herd," allowing scientists to ponder rather than search through candidates. In this research work, comprehensive in silico study was done to explore the possibilities of reusing statins as inhibitors of Histone deacetylase 3 (HDAC3), one of the epigenetic targets reported to be associated with breast cancer. With increased focus on drug repurposing to accelerate anticancer drug discovery, clinical anti-lipid agents are studied for their possible HDAC3 inhibitory activity. Molecular docking of selected statins (Atorvastatin, Fluvastatin, Pitavastatin, Pravastatin, and Rosuvastatin) was performed to study their energy of binding and binding cavity in HDAC3 catalytic pocket against Vorinostat as reference HDAC inhibitor. Special focus was on zinc coordination, hydrogen bonding, ionic interactions along with hydrophobic enclosure. In addition, exhaustive structure–activity relationships (SAR) were also reported. Additionally, a thorough in silico ADMET profiling was performed to study the pharmacokinetic properties, metabolic vulnerability, and safety properties of the compounds under study and other physicochemical descriptors and drug-likeness parameters.

2. Methods

2.1. Ligand Preparation

The chemical structures of the selected statins (Atorvastatin, Fluvastatin, Pitavastatin, Pravastatin, and Rosuvastatin) were retrieved from the PubChem database in SDF format. The reference inhibitor Vorinostat was taken as a reference. These ligands were energy minimized using appropriate force field parameters to obtain stable conformations prior to docking; protonation states were adjusted at physiological pH (7.4), and torsional bonds were defined to introduce conformational flexibility in docking.

2.2. Protein Preparation

The three-dimensional crystallographic structure of Histone deacetylase 3 (HDAC3) was retrieved from the Protein Data Bank (PBD ID: 4LXZ). To prepare the protein structure, co-crystallized ligands, water molecules, and all other heteroatoms attached to the protein were deleted. Polar hydrogen atoms were added, and Kollman charges were added to the appropriate atoms. The active site selection was based on the localization of the co-crystallized inhibitor and the ketamine catalytic zinc ion (Zn_2^+) which was retained for docking.

2.3. Molecular Docking Studies

Molecular docking studies were conducted to assess the binding mode and affinity of the selected statins within the catalytic pocket of HDAC3. Docking studies were performed using AutoDock (or appropriate docking software). A gridbox with dimension XX $\AA$ was generated and centred in the active site of XX. The key residues and the catalytic zinc ion were included. The binding energies (kcal·mol^{-1}), RMSD values etc. were recorded. The best docking poses were retained as those with the lowest binding energy and correct orientation in the active site. 2D and 3D interaction studies for hydrogen bonds, ionic interactions, π–π stackings and metal interactions were performed.

2.4. Structure Activity Relationship (SAR) Analysis

A comparative structure–activity relationship study was performed to determine structural factors influencing HDAC binding affinity. Particular emphasis was placed on zinc-binding groups, hydrophobic linker regions, aromatic cap structures, lipophilicity (LogP) , molecular flexibility (rotatable bonds) , and hydrogen bond donor/acceptor ability. These descriptors were correlated to docking scores in an attempt to rationalise binding trends.

2.5. ADMET Prediction

Pharmacokinetic and toxicity properties were predicted using in silico ADMET prediction tools (pkCSM, https://biosig.lab.uq.edu.au/pkcsm/).

2.6. Structure Activity Relationship (SAR)

The overall comparative structure activity relationship (SAR) between statins and Vorinostat suggests Figure 1 both similar mechanistic features and distinct structural elements modulating HDAC affinity. Vorinostat typifies a traditional HDAC pharmacophore, comprising (i) a hydroxamic acid zinc-binding group (ZBG), (ii) a hydrophobic aliphatic linker, and (iii) a surface recognition cap group. The hydroxamic acid group allows for bidentate chelation with the catalytic $Zn_2{}^+$ ion, accounting for a large part of its inhibitory ability. Statins are devoid of the hydroxamic acid, but have a carboxylate element in their dihydroxyheptanoic acid side chain, which seems to provide an alternative zinc-binding group. Docking results indicate that this carboxylate group may coordinate (ionic and metal interactions) with Zn401, likely in a monodentate fashion, suggesting a non-classical HDAC inhibition mechanism. Atorvastatin exhibited the strongest predicted binding of the statins, which is classically related to its increased lipophilicity along with a larger molecular surface area and greater number of rotatable bonds (larger hydrophobic enclosure shown in Figure 3) that help to mask the compound in the relatively narrow HDAC catalytic tunnel. These properties help mimic the Vorinostat linker–cap-style architecture. Multiple aromatic rings promote π–π stacking interactions with residues PHE and HIS and help stabilize the compound being held together inside the active site. The more hydrophilic statins with different polar substituents e.g. Pravastatin and L87Rosuvastatin exhibited relatively low docking scores due to the inability of the more polar compound to optimally penetrate the hydrophobic channel of the enzyme as effectively as its more lipophilic counterpart.

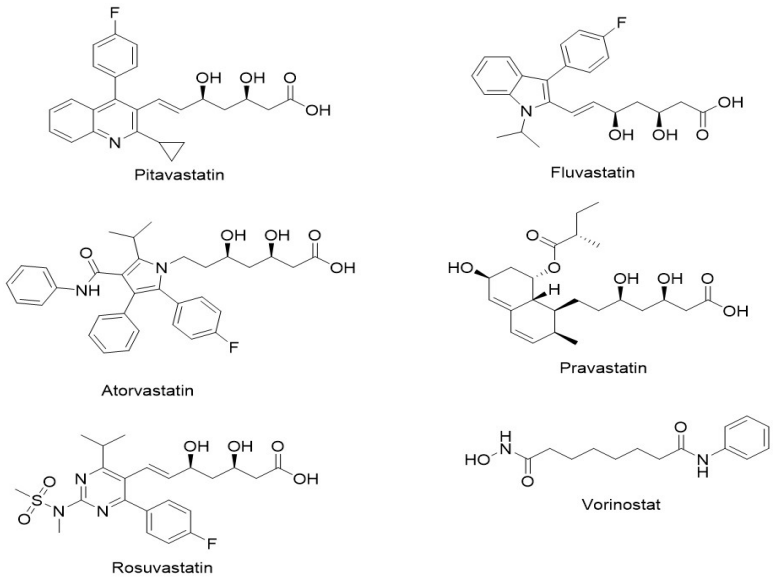

Figure 1: Chemical structure of statins and vorinostat drugs

The two statins Fluvastatin and Pitavastatin, which are of intermediate lipophilicity and contain aromatic scaffolds, displayed medium binding energies; this reflects the idea that a combination of some hydrophobicity and an aromatic character is useful for fitting into the HDAC pocket. In comparison to the linear and flexible aliphatic linker of Vorinostat, the statins are considerably bulkier and more rigid in that they possess rings, which may offer greater opportunity to interact in the cap-region, but may also present steric hindrance that interferes with an ideal geometry of similar zinc coordination as with the others in the active site. The conservation of the interactions with ASP181 and ASP269 in most statins suggests that electrostatic complementarity in the catalytic pocket is important for the stability of binding. Our evidence thus far points to the idea that the SAR seen for HDAC inhibition among the statins is driven by three major contributions: (i) Availability of the carboxylate zinc-binding group, (ii) Adequate hydrophobic surface area to fill the catalytic channel, and (iii) Aromatic moieties that can participate in π-interactions evident in at least the cap region. While Vorinostat benefits from optimal hydroxamic acid chelation, certain statins—most notably Atorvastatin—compensate through enhanced hydrophobic enclosure and multiple stabilizing interactions, elucidating their potential as non-hydroxamate HDAC inhibitor candidates. Further structural optimization, such as modification of the statin carboxylate to a more potent zinc-chelating group, may increase their inhibitory potency while improving selectivity toward desired HDAC isoforms.

2.7. Molecular Docking Studies

The molecular docking results confirmed that all of the statins tested were able to bind within the catalytic pocket of HDAC (PDB ID: 4LXZ) and make predicted interactions with the catalytic zinc ice (Zn401), much like the co-crystallized reference inhibitor Vorinostat Table 1. Among the statins tested, Atorvastatin exhibited an overall favorable docking affinity score of -10.93 kcal·mol^{-1}, which was better than the control Vorinostat (-8.51 kcal·mol^{-1}), with frequent stabilizing coordination of Zn401 (metal ion) in this case as well as many ionic contact interactions with ASP181 and ASP269, while also making sense of its tightly engaged hydrogen bonding with HIS145 as well as π-interactions with aromatic residues, to suggest that Atorvastatin is successfully occupying the active site of HDAC at least in silico. The remaining statins tested (Fluvastatin, Pitavastatin, Pravastatin, and Rosuvastatin) displayed a similar stable docking mode within HDAC with docking scores of -8.07 kcal·mol^{-1}, -7.99 kcal·mol^{-1}, -8.01 kcal·mol^{-1}, and -7.40 kcal·mol^{-1} respectively and RMSD values of under 2 $\AA$ confirming reliable docked poses for all the statins tested. Structure activity concept, perhaps, suggests that increasingly lipophilicity likely favored greater surface area and overall molecular flexibility like in the case of Atorvastatin may have permitted the greatest degree of increased hydrophobic enclosure of the molecules of the statins to the catalytic tunnel suggesting greater binding stability overall. ADMET profiling further strengthened the case for repurposing, with most statins exhibiting acceptably high intestinal absorption,

low BBB permeability, manageable metabolic profiles, and favorable toxicity predictions with respect to Vorinostat, albeit Atorvastatin indicated potential AMES positivity and hERG II inhibition. Altogether the consistent coordination/networking of zinc, conservation of interaction with the catalytic residue and reasonable pharmacokinetic profile offered good computational basis for statins being non-classical HDAC inhibitors Figure 2, 3, 4, 5 and 6.

Table 1: Molecular docking results of statins against 4LXZ

Ligand	**RMSD (Å)**	**Dock Score** $E, (\text{kcal} \cdot \text{mol}^{-1})$	**Interaction type**	**Residue / Partner**	**Δ E** $E, (\text{kcal} \cdot \text{mol}^{-1})$ **per interaction**	**Distance (Å)**
Atorvastatin	1.9471	-10.9269	Metal	ZN401	-3.2	1.86
			Ionic	HIS145	-4.3	3.02
			Ionic	ZN401	-19.2	1.86
			Ionic	ASP181	-4.9	2.93
			Ionic	ASP181	-21.2	1.77
			Ionic	ASP269	-21.9	1.74
			H-acceptor	HIS145	-5.9	3.02
			H-pi	PHE210	-0.6	3.96
Fluvastatin	1.2327	-7.4024	Metal	ZN401	-2.3	1.96
			Ionic	ASP181	-4.9	2.93
			Ionic	ASP181	-21.2	1.77
			Ionic	ASP269	-21.9	1.74
			H-acceptor	HIS145	-2.3	3.26
			H-pi	PHE155	-0.7	4.17
Pitavastatin	0.7722	-7.6607	Metal	ZN401	-2.3	2.07
			Ionic	ASP181	-4.9	2.93
			Ionic	ASP181	-21.2	1.77
			Ionic	ASP269	-21.9	1.74
			H-pi	HIS183	-0.6	3.64
Pravastatin	1.8832	-8.0734	Metal	ZN401	-2.9	1.98
			Ionic	ASP181	-4.9	2.93
			Ionic	ASP181	-21.2	1.77
			Ionic	ASP269	-21.9	1.74
			H-acceptor	ARG275	-0.4	3.28
Rosuvastatin	1.612	-7.777	Metal	ZN401	-0.7	2.69
			Ionic	ASP181	-4.9	2.93
			Ionic	ASP181	-21.2	1.77
			Ionic	ASP269	-21.9	1.74
			H-donor	HIS146	-1.1	2.96
			H-acceptor	TYR308	-1.8	3.05
			H-acceptor	GLY154	-0.6	3.24
Vorinostat	1.7676	-8.5099	Metal	ZN401	2.2	1.93
			Ionic	ASP181	-4.9	2.93
			Ionic	ASP181	-21.2	1.77
			Ionic	ASP269	-21.9	1.74
			H-acceptor	HIS145	-4.1	3.23
			H-pi	HIS183	-0.9	4.01
			pi-H	TYR209	-0.6	4.69

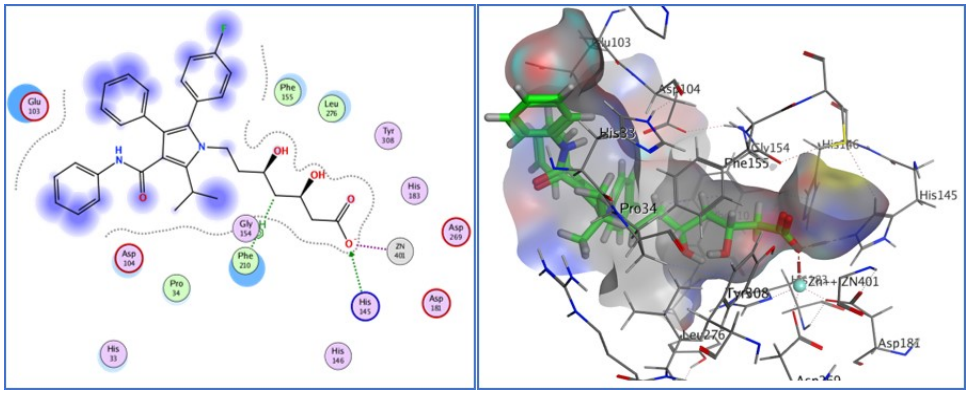

Figure 2: 2D & 3D Interaction between Atorvastatin with receptor (4LXZ)

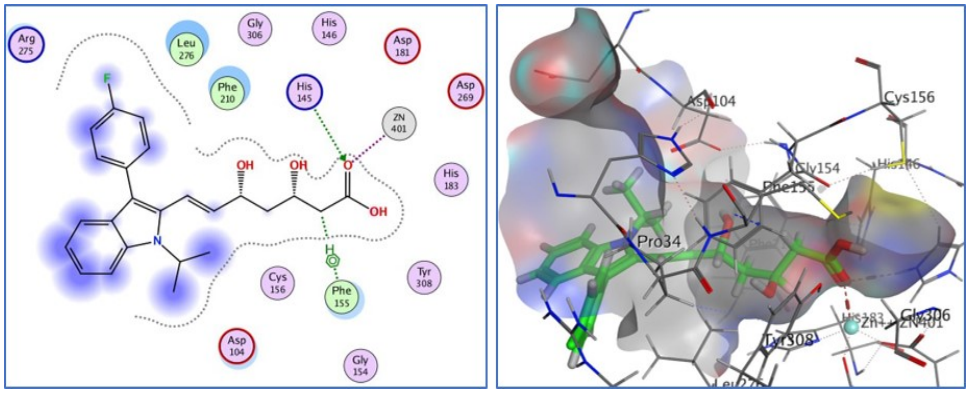

Figure 3: 2D & 3D Interaction between Fluvastatin with receptor (4LXZ)

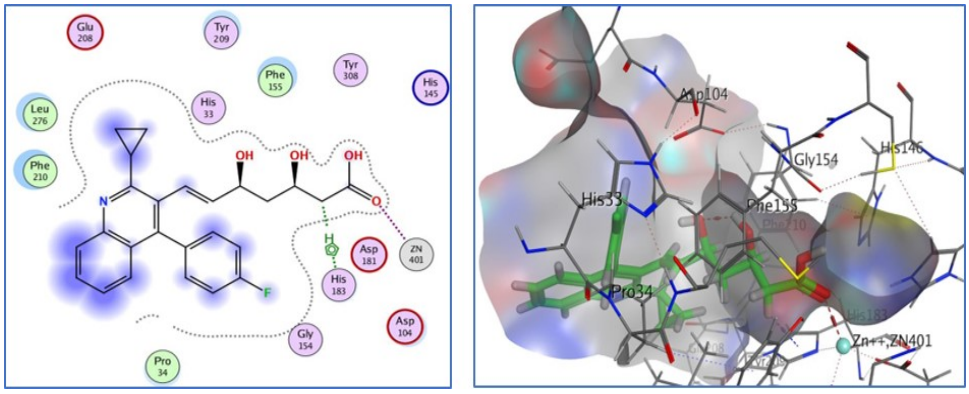

Figure 4: 2D & 3D Interaction between Pitavastatin with receptor (4LXZ)

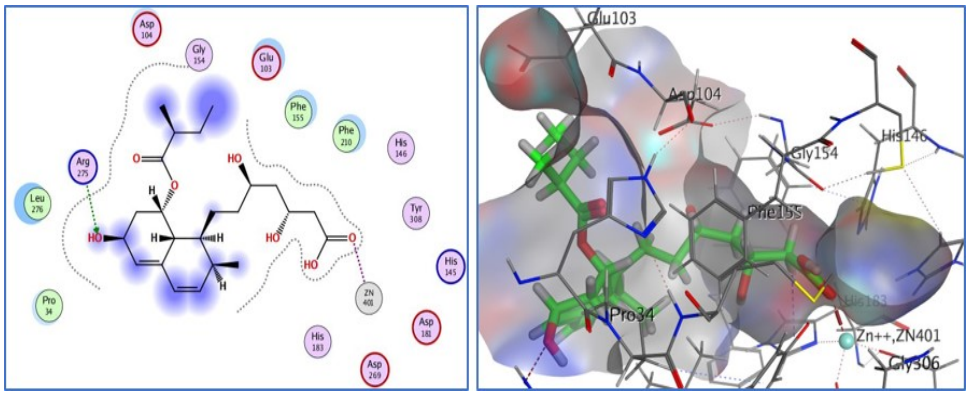

Figure 5: 2D & 3D Interaction between Pravastatin with receptor (4LXZ)

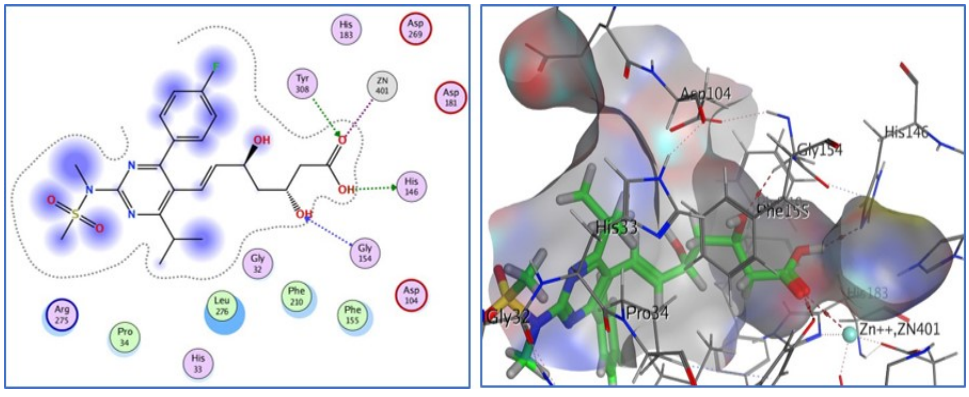

Figure 6: 2D & 3D Interaction between Rosuvastatin with receptor (4LXZ)

2.8. Pharmacokinetic Profile

The time course of a drug is termed its 'pharmacokinetic profile', a term referring to fate of the compound in the body as governed by absorption, distribution, metabolism, and elimination (i.e. the "ADME" processes which underlie its concentration–time profile). All these attributes are much desired within drug discovery and repurposing; they critically influence therapeutic action, application, dose frequency, and likelihood of adverse drug–drug interactions (even compounds which bind powerfully at their chosen target, can fail in clinical development if their pharmacokinetic/fate physical properties are suboptimal).

2.9. Absorption Prediction Profile: Statins vs Vorinostat

The in silico absorption analysis presented differences in predicted pharmacokinetics between the statins and Vorinostat. Vorinostat is predicted to have moderate aqueous solubility (log mol/L -2.67) and high predicted intestinal absorption (91.64%), reflecting its relatively balanced polarity and molecular weight Table 2. By contrast, the evaluated statins displayed lower predicted values of water solubility (-3.40 to -4.81 log mol/L range), commensurate with their larger molecular weights and greater lipophilicity. The somewhat lower solubility predicted for several of the statins results in excellent predicted human intestinal absorption which exceeds that of Vorinostat for Fluvastatin (93.33%) and Pitavastatin (95.41%) etc. suggesting that a more lipophilic structure may lead to better passive membrane permeability despite lower aqueous solubility characteristics. Predicted **Caco$_2$** permeability for the statins showed differences in comparison to Vorinostat; Fluvastatin (0.654) and Pravastatin (0.593) is similar to Vorinostat (0.609), however Atorvastatin has a lower predicted permeability (-0.328), perhaps reflecting its larger molecular weight and more complex structure. Rosuvastatin had lower permeability (0.091) presumably reflecting its greater polarity and presence of further hydrogen bonds donors & acceptors, meaning limited passive diffusion across epithelial membranes in the intestine. Permeability through skin was similar for all compounds. None of the statins were predicted to act as inhibitors of P-glycoprotein I, so there would not be a concern with respect to reduced absorption via efflux. However, most statins were predicted to be substrates for P-glycoprotein which may lead to variations in absorption kinetics and exposure profiles. Overall, the absorption observation suggests that although statins have lower aqueous solubility than Vorinostat in general, their overall high predicted intestinal absorption especially for the more lipophilic compounds provides reassurance regarding their bioavailability. The balance between lipophilicity and polarity seems to be the key to absorption performance, with moderately lipophilic statins displaying optimal permeability properties. Together these results underline feasibility for dosing of statins as orally active HDAC inhibitors, albeit with the need for further structure optimization to enhance the solubility permeability balance.

Table 2: In Silico Absorption Prediction Profile of the statins Compared with Vorinostat

Model Name	Pitavastatin	Fluvastatin	Atorvastatin	Pravastatin	Rosuvastatin	Vorinostat	Unit
Water solubility	-4.81	-4.649	-3.401	-3.575	-4.454	-2.672	Numeric (log mol/L)
Caco2 permeability	0.454	0.654	-0.328	0.593	0.091	0.609	Numeric (log Papp in 10^{-6} cm/s)
Intestinal absorption (human)	95.41	93.334	67.994	49.515	46.757	91.64	Numeric (% Absorbed)
Skin Permeability	-2.735	-2.735	-2.735	-2.75	-2.736	-2.835	Numeric (log Kp)
P-glycoprotein substrate	Yes	Yes	Yes	Yes	Yes	No	Categorical (Yes/No)
P-glycoprotein I inhibitor	No	No	No	No	No	No	Categorical (Yes/No)
P-glycoprotein II inhibitor	No	YES	YES	No	No	No	Categorical (Yes/No)

2.10. Distribution Prediction Profile

The analysis of the in silico distribution revealed significant differences between Vorinostat and statins, which were primarily a product of size of the compound, lipophilicity and the tendency to bind plasma proteins Table 3. Vorinostat had a predicted VDss of -0.54 log L/kg, indicating moderate distribution to tissues (/ Vss of approximately 3L) while the statins were predicted to have lower VDss values (-0.85 to -1.93 log L/kg). Atorvastatin had the lowest VDss values (-1.929), consistent with higher lipophilicity and extensive ($\geq$ 80%) plasma protein binding which would restrict free distribution in serum. This is also reflected in the Fu values of these compounds. Vorinostat had a higher unbound fraction (0.263) meaning more of the drug is free to bind to its target. In stark contrast Fluvastatin (0.0) and Pitavastatin (0.027) had very low Fu values indicating this compound is highly protein bound. The more the compound is associated with the protein the less of it will be free in the bloodstream. That said, highly protein bound drugs are unlikely to be available as quickly as their unbound counterparts but can remain in the blood circulation longer; retaining a longer half-life, which can contribute to a longer pharmacological action.

In terms of blood–brain barrier (BBB) permeability (predicted logBB $<$-1 for all compounds), all compounds would have limited ability to penetrate the CNS. Rosuvastatin had the lowest BBB permeability (-2.037), which might be consistent with a higher polarity and number of potential hydrogen bond donors. Vorinostat consequently also has restricted BBB penetration (-1.093) suggesting that both

the reference inhibitor and statins are mainly peripherally distributed agents, a positive feature for limiting CNS adverse effects during systemic anticancer therapy. CNS permeability (log PS) predictions were also low for all molecules with Rosuvastatin predicted to have the most restricted permeability (-4.042) while Fluvastatin is predicted to have relatively greater CNS penetration (-2.468). It appears that lipophilicity is only a moderating influence on central distribution, structural polarity and MW provide greater limits. Taken together, the distribution profile indicates that Vorinostat has moderate systemic and tissue distribution and higher free fraction, whereas the statins are plasma protein-bound/have a lower tissue distribution (but adequate availability to peripheral tissues), and both have poor BBB penetration (making them viable in non-CNS oncology). These pharmacokinetic properties (in conjunction with the docking results) add to the feasibility of the statins as potential repurposed HDAC inhibitors, with the understanding that protein binding effects need to be factored into assessed effective concentrations.

Table 3: In Silico Distribution Prediction Profile of the statins Compared with Vorinostat

Model Name	Pitavastatin	Fluvastatin	Atorvastatin	Pravastatin	Rosuvastatin	Vorinostat	Unit
VDss (human)	-1.409	-0.959	-1.929	-1.044	-0.85	-0.54	Numeric (log L/kg)
Fraction unbound (human)	0.027	0	0.1	0.349	0.162	0.263	Numeric (Fu)
BBB permeability	-1.113	-1.043	-1.392	-1.067	-2.037	-1.093	Numeric (log BB)
CNS permeability	-3.101	-2.468	-2.84	-3.513	-4.042	-3.039	Numeric (log PS)

2.11. Metabolism Prediction Profile

In silico metabolism prediction results indicate differences in the interactions of statins and Vorinostat with cytochrome P450 (CYP450) enzymes, highlighting structural complexity and clinical indication Table 4. Vorinostat was predicted to be a CYP3A4 substrate, consistent with hepatic metabolism, and to show no inhibitory behavior toward the remaining relevant CYP isoforms evaluated, CYP1A2, CYP2C19, CYP2C9, CYP2D6, and CYP3A4. This suggests a relatively low expectation for metabolic drug–drug interactions. Among the statins, Atorvastatin was predicted to be both a CYP3A4 and CYP2D6 substrate and an inhibitor of CYP2C19 and CYP2C9. This greater metabolic promiscuity suggests a higher likelihood of metabolic involvement and potential drug–drug interactions, and is occurent with its high lipophilicity and complex aromatic structure. Fluvastatin and Pitavastatin were also predicted as CYP3A4 substrates, with Fluvastatin additionally a CYP2C19 inhibitor aspiring moderate metabolic liability. Rosuvastatin and Pravastatin were not predicted as CYPD6 or CYP3A4 substrates and had low predicted inhibitory capability, suggesting simpler metabolic behavior and potentially lower risk for drug interactions. Vorinostat itself was not acted upon by CYP 1A2 or CYP2D6. The statins show variability in CYP interactions that appears to be correlated with lipophilicity and bulk, with more lipophilic agents (e.g. at least atorvastatin) exhibiting broader concentrations of CYP involvement. Overall, while Vorinostat has a relatively simple metabolic profile and demonstrates limited CYP inhibition, some statins especially Atorvastatin could potentially be more at risk for metabolic interactions; however, since they are already in clinical use with well understood hepatic metabolism pathways, this information may actually bolster the case for their repurposing as proven therapeutics since recommended dose adjustments and potential metabolic interaction risks are already known. Overall, it appears from a metabolic perspective that most statins generate acceptable in silico profiles, although consideration of CYP interactions will be critical when developing future HDAC-targeted therapeutics.

Table 4: In Silico Metabolism Prediction Profile of the statins Compared with Vorinostat

Model Name	Pitavastatin	Fluvastatin	Atorvastatin	Pravastatin	Rosuvastatin	Vorinostat	Unit
CYP2D6 substrate	No	No	Yes	No	No	No	Categorical (Yes/No)
CYP3A4 substrate	Yes	Yes	Yes	No	No	Yes	Categorical (Yes/No)
CYP1A2 inhibitior	No	No	No	No	No	No	Categorical (Yes/No)
CYP2C19 inhibitior	No	Yes	Yes	No	No	No	Categorical (Yes/No)
CYP2C9 inhibitior	Yes	Yes	Yes	No	No	No	Categorical (Yes/No)
CYP2D6 inhibitior	No	No	No	No	No	No	Categorical (Yes/No)
CYP3A4 inhibitior	No	No	No	No	No	No	Categorical (Yes/No)

2.12. In Silico Excretion Prediction Profile

The differences observed in the in silico analysis of excretion suggest that statins and Vorinostat will have differences in predicted total clearance and renal transport properties and that this is largely modulated by the MW, lipophilicity and plasma protein binding characteristics of the options Table 5. Vorinostat has a predicted total clearance value of 0.438 log ml/min/kg indicating moderate systemic elimination. Rosuvastatin and Pravastatin show higher predicted total clearance value, suggesting faster systemic elimination and therefore possibly a shorter half-life than Vorinostat would have at the same dosing regimens. Pitavastatin is between Vorinostat and Rosuvastatin in clearance. Atorvastatin and Fluvastatin exhibit the lowest predicted clearance values suggesting these two drugs will have slower systemic elimination, which is correlated with the higher lipophilicity and stronger plasma protein binding characteristics exhibited in the distribution profile

above. This lower clearance predicted for Atorvastatin would mean it could have prolonged systemic exposure which would be useful for persistence of HDAC inhibition but it may also carry the increased potential for accumulation depending on dosing schedules chosen. In a different vein, the higher clearance predicted for Rosuvastatin and Pravastatin compounds may result in a lower risk of accumulation, but may necessitate a higher or increase-frequency dosing schedule in the event they are repurposed for anticancer activity. None of the compounds analysed including Vorinostat exhibit a predicted active transport substrate-like behaviour for the renal organic cation transporter 2 (OCT2) - renal active secretion via this transporter is therefore not likely to play a significant role in their elimination, and as such hepatic metabolism and biliary excretion are likely to serve are the dominant elimination routes, particularly for the more lipophilic statins. The lipophilic statins (e.g., atorvastatin and fluvastatin) tend to have lower predicted clearances (consistent with sustained pharmacological action across periods of time), whereas the more hydrophilic statins (e.g., rosuvastatin and pravastatin) tend to have higher clearances: great care needs to be taken if these drugs are tagged for repurposing as HDAC inhibitors, and this suggests that modelling would need to be done with respect to their pharmacokinetics and dosing schedules.

Table 5: In Silico Excretion Prediction Profile of the statins Compared with Vorinostat

Model Name	Pitavastatin	Fluvastatin	Atorvastatin	Pravastatin	Rosuvastatin	Vorinostat	Unit
Total Clearance	0.784	0.417	0.229	1.238	1.407	0.438	Numeric (log ml/min/kg)
Renal OCT2 substrate	No	No	No	No	No	No	No

2.13. In Silico Toxicity Prediction Profile

The in silico prediction profile of the statins compared with Vorinostat shows notable data for several parameters Table 6. None of the compounds (except Atorvastatin) are predicted to be AMES toxic thus suggesting that compared to Vorinostat statins are mutagenic. The maximum tolerated dose (human) predictions are relatively low for Pravastatin (-0.092 log mg/kg/day) and Rosuvastatin (-0.02 log mg/kg/day) as opposed to Vorinostat and Fluvastatin that show higher tolerated doses. For cardiac safety, none of the compounds are predicted to be hERG I inhibitors while only Atorvastatin predicted to be hERG II inhibitor, suggesting at least a moderate risk for cardiac arrhythmias. Acute oral toxicity (LD50), (that is, predicted value in rats) is highest for Rosuvastatin (3.608 mol/kg) and lowest for Pravastatin (1.908 mol/kg). Chronic toxicity predictions (LOAEL) were highest for Atorvastatin (4.019 log mg/kg_ bw/day), with Pitavastatin being the lowest, reflecting potential differences in the safety of long-term exposures. Hepatotoxicity was predicted for Rosuvastatin, Atorvastatin, Fluvastatin, and Pitavastatin indicating a possible risk of liver toxicity with these compounds, whereas Vorinostat, Pravastatin, and Fluvastatin were not predicted to cause skin sensitization. Pyriformis toxicity (environmental) was all relatively low for these, but Minnow toxicity ranged from -3.151 log mM for Atorvastatin strongly negative indicating higher predicted aquatic toxicity, to least effect 3.181 log mM for Vorinostat. In summary, these in silico predictions may show that whilst these statins fall within a relatively safe profile to Vorinostat, there may be concerns regarding hepatotoxicity, cardiac risk, and environmental impacts particularly found in Atorvastatin.

Table 6: In Silico Toxicity Prediction Profile of the statins Compared with Vorinostat

Model Name	Pitavastatin	Fluvastatin	Atorvastatin	Pravastatin	Rosuvastatin	Vorinostat	Unit
AMES toxicity	No	No	Yes	No	No	No	Categorical (Yes/No)
Max. tolerated dose (human)	0.076	0.459	0.323	-0.092	-0.02	1.134	Numeric (log mg/kg/day)
hERG I inhibitor	No	No	No	No	No	No	Categorical (Yes/No)
hERG II inhibitor	No	No	Yes	No	No	No	Categorical (Yes/No)
Oral Rat Acute Toxicity (LD50)	2.191	2.708	2.774	1.908	3.608	2.609	Numeric (mol/kg)
Oral Rat Chronic Toxicity (LOAEL)	0.907	2.739	4.019	1.577	2.478	2.007	Numeric (log mg/kg_bw/day)
Hepatotoxicity	Yes	Yes	Yes	No	Yes	No	Categorical (Yes/No)
Skin Sensitisation	No	No	No	No	No	No	Categorical (Yes/No)
T.Pyriformis toxicity	0.286	0.295	0.285	0.302	0.291	0.342	Numeric (log ug/L)
Minnow toxicity	-0.576	-0.311	-3.151	2.69	0.939	3.181	Numeric (log mM)

2.14. Physicochemical Descriptors

Comparative analysis of physicochemical properties and drug-likeness descriptors for the statins compared to Vorinostat Table 7 shows a few highlights related to factors of pharmacokinetics and molecular flexibility: Vorinostat has the lowest molecular weight (264.33 g/mol) while Atorvastatin is the heaviest (558.65 g/mol), which may have effects on absorption and bioavailability. The values for Log P lipidic liveliness show Vorinostat (2.47) and Rosuvastatin (2.40), much less lipophilic than Atorvastatin (6.31) and Fluvastatin (4.63), suggesting

that the later are more likely to cross membranes but may also be less soluble in normal water phase. All compounds have a moderate to a high number of rotatable bonds, with Atorvastatin having the most (12), indicating a tendency for greater flexibility which may enhance receptor binding and oral bioavailability. All the statins have a relatively consistent number of hydrogen bond acceptors and donors, with a generally higher count for Atorvastatin and Pravastatin (5–6) enhancing attractiveness to polar environments or targets. Surface area levels are commensurate with the size of the molecules as Vorinostat has the smallest surface area (112.52 $Å^2$) while Atorvastatin is the largest (238.46 $Å^2$), potentially indicating that larger statins may have additional steric hindrance preventing effective binding or transport. Overall these descriptors suggest that while all statin drugs conform to a general drug-likeness level, molecular weight, lipophilicity and flexibility may influence distribution/human absorption and interaction with Vorinostat.

Table 7: Physicochemical Properties and Drug-Likeness Descriptors of the statins Compared with Vorinostat

Descriptor	Rosuvastatin	Pravastatin	Atorvastatin	Fluvastatin	Pitavastatin	Vorinostat
Molecular Weight	481.546	424.534	558.65	411.473	421.468	264.325
LogP	2.4017	2.4404	6.3136	4.6281	4.5181	2.4711
Rotatable Bonds	10	10	12	8	8	8
Acceptors	7	6	5	4	4	3
Donors	3	4	4	3	3	3
Surface Area	191.848	177.991	238.457	174.259	179.054	112.522

3. Conclusions

In conclusion, the current study highlights the feasibility of statins as repurposed molecules inhibiting Histone deacetylase 3 utilising an in silico approach complementing molecular docking, structure activity relationship (SAR) and ADMET profiling. All statin compounds occupy the catalytic pocket of HDAC3 and share common interaction with the catalytic Zn_2ion similar to the positive control Vorinostat. However, of the statins evaluated, Atorvastatin demonstrated the best binding affinity and interaction stability attributed to high hydrophobic enclosure, good aromatic π–interactions and zinc coordination. Each other statin demonstrated moderate binding continuation with stability confirming that the statin scaffold can conduct as a non-classical zinc binding moiety. SAR analysis showed that lipophilicity and aromatic nature and accessibility of the carboxylate group is required to stabilise interactions down the HDAC catalytic tunnel. ADMET prediction shows that most statins have acceptable absorption, distribution, metabolism and excretion profiles due to their status of therapeutic agents. Although some of these compounds may constitute a concern (Atorvastatin for example predicted AMES positivity or hERG II inhibition), the overall safety profiles remain favourable in comparison to many new experimental inhibitors. Taken together, these finding suggest the possibility that STATTICs could be repurposed as epigenetic anticancer agents inhibiting HDAC3. Confirmation through in vitro enzymatic assays, cellular studies, and in vivo models will be required to show their inhibitory potency, selectivity, and/or therapeutic potential in breast cancer.

Article Information

Disclaimer (Artificial Intelligence): The author(s) hereby declare that NO generative AI technologies such as Large Language Models (ChatGPT, COPILOT, etc.), and text-to-image generators have been used during writing or editing of manuscripts.

Competing Interests: Authors have declared that no competing interests exist.

References

[1] W. Cao, H.-D. Chen, . Y.-W. Yu, N. Li, and W.-Q. Chen. Changing profiles of cancer burden worldwide and in China: a secondary analysis of the global cancer statistics 2020. *Chin. Med. J.*, 134(7):783–791, 2021. URL https://doi.org/10.1097/%20CM9.0000000000001474.

[2] M. Arnold, E. Morgan, H. Rumgay, A. Mafra, D. Singh, M. Laversanne, J. Vignat, J.R. Gralow, F. Cardoso, S. Siesling, and I. Soerjomataram. Current and future burden of breast cancer: global statistics for 2020 and 2040. *Breast*, 66(66), 2022. URL https://doi.org/10.1016/j.breast.2022.08.010.

[3] D. Guo, L. Kong, J. Liu, L. Zhan, L. Luo, W. Zheng, Q. Zheng, C. Chen, and S. Sun. Breast cancer heterogeneity and its implication in personalized precision therapy. *Exp. Hematol. Oncol.*, 12(1):3, 2023. URL https://doi.org/10.1186/s40164-022-00363-1.

[4] W. Jin, Q.-Z. Li, Y. Liu, and Y.-C. Zuo. Effect of the key histone modifications on the expression of genes related to breast cancer. *Genomics*, 112(1):853–858, 2020. URL https://doi.org/10.1016/j.ygeno.2019.05.026.

[5] M. Yoshida, N. Kudo, S. Kosono, and A. Ito. Chemical and structural biology of protein lysine deacetylases. In *Proc. Japan Acad. Series B 93 (5)*, pages 297–321, 2017. URL https://doi.org/10.2183/pjab.93.019.

[6] Z. Cui, M. Xie, Z. Wu, and Y. Shi. Relationship between histone deacetylase 3 (HDAC3) and breast cancer. *Med. Sci. Monit.*, 24: 2456–2464, 2018. URL https://doi.org/10.12659/msm.906576.

[7] H.-C. Kim, K.C. Choi, H.K. Choi, H.K. Kang, M.J. Kim, Y.H. Lee, O.H. Lee, J. Lee, Y.J. Kim, W. Jun, J.W. Jeong, and H.G. Yoon. HDAC3 selectively represses CREB3-mediated transcription and migration of metastatic breast cancer cells. *Cell. Mol. Life Sci.*, 67 (20):3499–3510, 2010. URL https://doi.org/10.1007/s00018-010-0388-5.

[8] R. Rahbari, Y. Rasmi, M. H. Khadem-Ansari, and M. Abdi. The role of histone deacetylase 3 in breast cancer. *Med. Oncol.*, 39(7): 22–01681, 2022. URL https://doi.org/10.1007/s12032-022-01681-4.

[9] X. Qiu et al. From natural products to HDAC inhibitors: an overview of drug discovery and design strategy. *Bioorg. Med. Chem.*, 52: 116510, 2021. URL https://doi.org/10.1016/j.bmc.2021.116510.

[10] I. P. Singh, F. Ahmad, D. Chatterjee, R. Bajpai, and N. Sengar. Natural products: drug discovery and development. *Drug Discov. Dev.*, 2:11–65, 2021. URL https://doi.org/10.1007/978-981-15-5534-3_2.

[11] T. T. Ashburn and K. B. Thor. Drug repositioning: identifying and developing new uses for existing drugs. *Nat. Rev. Drug Discov.*, 3 (8):673–683, 2004. URL https://doi.org/10.1038/nrd1468.